URSI GASS 2021, Rome, Italy, 28 August - 4 September 2021

Generalised Self-Holography

Stefan J. Wijnholds
Netherlands Institute for Radio Astronomy (ASTRON), Dwingeloo, The Netherlands
Dept. Electrical and Electronic Engineering, Stellenbosch University, Stellenbosch, South Africa

Abstract

The recently proposed self-holography method has the potential to reduce the computational resources needed for calibration of individual receive paths in large arrays like LOFAR and SKA significantly. The method relies on forming different beams from which the receive path gains can be reconstructed. Self-holography has been applied successfully with different beamforming schemes. In this contribution, I present a generalised formulation of self-holography capturing any beamforming scheme and use that to assess its robustness to interfering sources. This analysis indicates that the relative gain bias is inversely proportional to the signal-to-interference ratio (SIR) regardless of the beamforming scheme used. This result is corroborated in simulations. However, the chosen beamforming scheme has significant impact on the condition number of the measurement matrix and, hence, on the susceptibility to measurement noise. A beamforming scheme with (nearly) orthogonal beamformer weight vectors is thus to be preferred.

1 Introduction

Calibration of radio astronomical arrays usually involves measuring the visibilities, i.e., the array covariance matrix. For this, the number of measurements scales quadratically with the number of elements in the array. This can be computationally impractical for large arrays. A technique dubbed self-holography was proposed to remedy this [1]. This technique assumes that the output of a reference beam pointed at a strong calibration source is correlated with the signals from the individual receiving elements in the array, making the number of measurements scale linearly with the number of receiving elements. It is assumed that the reference beam provides sufficient isolation of the signal from the calibration source to ignore the presence of other sources. The impact of the signal-to-interference ratio (SIR) on the quality of the calibration solutions was studied in depth in [2] leading to the conclusion that self-holography can provide gain estimates of sufficient quality for a number of practical scenarios, including (initial) calibration of the stations of the Low Frequency Array (LOFAR) [3]. This conclusion was further corroborated by an experiment to calibrate a prototype station for the low-frequency aperture array system of the Square Kilometre Array (SKA) [4] using self-holography on the Sun [5]. In this experiment, however, the output of the reference beam was correlated with the output of beams pointed towards a grid of points on the sky instead of the output of individual elements. This poses the question whether this improves the robustness of self-holography to interfering sources.

In this contribution, I present results from a first exploration of this problem. Noting that the signal from individual elements can be obtained by beamforming the array such that all beamformer weights are set to zero except for one particular element, I start by generalising the self-holography measurement equation, or data model, to describe a measurement in which the output of the reference beam is correlated with the output signals from multiple beams. I then use this data model to derive an expression for the impact of the SIR on the gain estimation bias in generalised self-holography in Sec. 3 analogous to the derivation in [2]. This expression is corroborated by the simulations presented in Sec. 4 before summarising the conclusions.

2 Data model

The array consisting of P receiving elements is assumed to receive Q narrowband sources. The signal from the qth source is modelled by a time series $s_q(t)$. The signal from all sources can thus be stacked in a $Q \times 1$ vector $\mathbf{s}(t)$. As the signals are assumed to be narrowband, the arrival time differences between the receiving elements can be modelled by phasors. Also, each receiving element may have a different gain towards each source. The multiplication of these two factors results in a complex valued gain factor per receiving element per source a_{pq}, which can be collected in a $P \times Q$ matrix $\mathbf{A}$. The gains of the analog receive paths between the antenna output ports and the analog-to-digital converters, g_p can be stacked in a $P \times 1$ vector $\mathbf{g}$. Adding additive noise to each receive path, described by the $P \times 1$ noise vector $\mathbf{n}(t)$, gives the array signal vector

$$\mathbf{x}(t) = \mathbf{G}\mathbf{A}\mathbf{s}(t) + \mathbf{n}(t), \tag{1}$$

where $\mathbf{G} = \mathrm{diag}(\mathbf{g})$ is a diagonal matrix with the receive path gains on the main diagonal.

The output of the kth beamformer can be described by $y_k(t) = \mathbf{w}_k^H \mathbf{x}(t)$, where the $P \times 1$ vector $\mathbf{w}_k$ contains the

beamformer weights and ^{H} denotes the Hermitian transpose. Note that if weights are set to zero except one, which is set to unity, the beamformer can select the output signal of a specific element. The weights for K beamformers can be stacked in a matrix $W = [\mathbf{w}_1, \cdots, \mathbf{w}_K]$ such that the output signals of the K beamformers can be described by the $K \times 1$ vector

$$\mathbf{y}(t) = \mathbf{W}^H \mathbf{x}(t) = \mathbf{W}^H \mathbf{G}\mathbf{A}\mathbf{s}(t) + \mathbf{W}^H \mathbf{n}(t). \quad (2)$$

In generalised self-holography, these output signals are correlated with the output signal from the reference beam $y_{\text{ref}}(t) = \mathbf{w}_{\text{ref}}^H \mathbf{x}(t)$. The expected value of these $K \times 1$ correlations is

$$\begin{aligned} \mathbf{r}_{\text{ref}} &= \mathscr{E}\left\{\mathbf{y}(t) y_{\text{ref}}^H(t)\right\} \\ &= \mathbf{W}^H \mathbf{G} \Sigma_{\text{s}} \mathbf{G}^H \mathbf{w}_{\text{ref}} + \mathbf{W}^H \Sigma_{\text{n}} \mathbf{w}_{\text{ref}}, \end{aligned} \quad (3)$$

where Σ_{s} and Σ_{n} represent the covariance matrices of the source signals and the noise signals, respectively, which are assumed to be mutually uncorrelated. Using the Khatri-Rao product, the column-wise Kronecker product denoted by $\circ$, and the fact that $\mathbf{G} = \text{diag}(\mathbf{g})$ and $\Sigma_{\text{n}} = \text{diag}(\sigma_{\text{n}})$, we can write this as

$$\mathbf{r}_{\text{ref}} = \left(\left(\Sigma_{\text{s}} \mathbf{G}^H \mathbf{w}_{\text{ref}}\right)^T \circ \mathbf{W}^H\right) \mathbf{g} + \mathbf{W}^H \text{diag}(\mathbf{w}_{\text{ref}}) \sigma_{\text{n}}. \quad (4)$$

Self-holography as described in [2] also uses the autocorrelations of the output signals from the individual receiving elements to apply appropriate corrections for the noise power in the measurements. Although it seems natural to generalise this to the autocorrelations of the beamformer output signals, this will usually lead to an ill-conditioned problem due to the fact that all beamformers form very similar superpositions of the noise powers of the individual receiving elements. It is therefore better to measure the autocorrelations of the output signals from the individual receive paths. In most radio interferometers, this is the case as they are commonly used for diagnostic purposes. These autocorrelations can be described by the $P \times 1$ vector [2]

$$\begin{aligned} \mathbf{r}_{\text{ac}} &= \text{vecdiag}\left(\mathscr{E}\left\{\mathbf{x}(t)\mathbf{x}^H(t)\right\}\right) \\ &= \text{diag}\left(\text{vecdiag}\left(\Sigma_{\text{s}} \mathbf{G}^H\right)\right) \mathbf{g} + \sigma_{\text{n}}, \end{aligned} \quad (5)$$

where $\text{vecdiag}(\cdot)$ converts the main diagonal of a matrix into a column vector and $\text{diag}(\cdot)$ converts a vector into a square diagonal matrix with the elements of the vector on its main diagonal.

By stacking (4) and (5), we obtain

$$\begin{aligned} \begin{bmatrix} \mathbf{r}_{\text{ref}} \\ \mathbf{r}_{\text{ac}} \end{bmatrix} &= \begin{bmatrix} \left(\Sigma_{\text{s}} \mathbf{G}^H \mathbf{w}_{\text{ref}}\right)^T \circ \mathbf{W}^H & \mathbf{W}^H \text{diag}(\mathbf{w}_{\text{ref}}) \\ \text{diag}\left(\text{vecdiag}\left(\Sigma_{\text{s}} \mathbf{G}^H\right)\right) & \mathbf{I} \end{bmatrix} \begin{bmatrix} \mathbf{g} \\ \sigma_{\text{n}} \end{bmatrix} \\ &= \begin{bmatrix} \mathbf{M}_{11} & \mathbf{M}_{12} \\ \mathbf{M}_{21} & \mathbf{M}_{22} \end{bmatrix} \begin{bmatrix} \mathbf{g} \\ \sigma_{\text{n}} \end{bmatrix} = \mathbf{M}\theta, \end{aligned} \quad (6)$$

where $\mathbf{I}$ denotes the identity matrix. This is the measurement equation for generalised self-holography, which should be inverted to obtain estimates for the receive path gains and noise powers from the measurements. If the measurement matrix is not invertible, this implies that the chosen set of K beams is not suitable for self-holography. As a minimum requirement, we need $K \geq P$. If $\mathbf{W}$ is equal to the identity matrix, the measurement equation simplifies to the measurement equation for self-holography based on the correlations with the signals from individual receiving elements as described in [2].

3 SIR for generalised self-holography

When inverting (6), we can identify two scenarios: $K = P$ and $K > P$. in the first case, $\mathbf{M}$ is a square matrix and its inverse can be calculated using

$$\mathbf{M}^{-1} = \begin{bmatrix} \mathbf{S}^{-1} & -\mathbf{S}^{-1}\mathbf{M}_{12}\mathbf{M}_{22}^{-1} \\ -\mathbf{M}_{22}^{-1}\mathbf{M}_{21}\mathbf{S}^{-1} & \mathbf{M}_{22}^{-1} + \mathbf{M}_{22}^{-1}\mathbf{M}_{21}\mathbf{S}^{-1}\mathbf{M}_{12}\mathbf{M}_{22}^{-1} \end{bmatrix}, \quad (7)$$

where $\mathbf{S} = \mathbf{M}_{11} - \mathbf{M}_{12}\mathbf{M}_{22}^{-1}\mathbf{M}_{21}$. In the second case, the Moore-Penrose pseudo-inverse can be used, i.e., $\mathbf{M}^\dagger = (\mathbf{M}^H\mathbf{M})^{-1}\mathbf{M}^H$. Assuming that all beams are formed simultaneously, forming more than P superpositions of the P input signals should not provide additional information. I will therefore focus on the case $K = P$ and use it to assess the implications of (7) in the context of interfering sources. The simulations presented in the next section will corroborate this reasoning by showing that similar results are obtained for $K > P$.

Combining (7) with (6), we find that, for $K = P$,

$$\mathbf{g} = \mathbf{S}^{-1}\left(\mathbf{r}_{\text{ref}} - \mathbf{W}^H \text{diag}(\mathbf{w}_{\text{ref}})\mathbf{r}_{\text{ac}}\right). \quad (8)$$

Following the same reasoning as in [2], we split the source covariance matrix in a contribution from the calibration source, Σ_{c}, and a contribution from the interfering sources, Σ_{int}. Substitution of (3) and (5) in (8) with $\Sigma_{\text{s}} = \Sigma_{\text{c}} + \Sigma_{\text{int}}$ while ignoring the noise contribution gives

$$\begin{aligned} \mathbf{g} = \mathbf{S}^{-1}\Big(&\mathbf{W}^H\widetilde{\mathbf{G}}\Sigma_{\text{c}}\widetilde{\mathbf{G}}^H\mathbf{w}_{\text{ref}} + \mathbf{W}^H\widetilde{\mathbf{G}}\Sigma_{\text{int}}\widetilde{\mathbf{G}}^H\mathbf{w}_{\text{ref}} + \\ &-\mathbf{W}^H\text{diag}(\mathbf{w}_{\text{ref}})\text{vecdiag}\left(\widetilde{\mathbf{G}}\Sigma_{\text{c}}\widetilde{\mathbf{G}}^H\right) + \\ &-\mathbf{W}^H\text{diag}(\mathbf{w}_{\text{ref}})\text{vecdiag}\left(\widetilde{\mathbf{G}}\Sigma_{\text{int}}\widetilde{\mathbf{G}}^H\right)\Big) \end{aligned} \quad (9)$$

where $\widetilde{\mathbf{G}}$ denotes the true values of the gains. As shown in [2], iterative application of this solution converges to the true gain values in the absence of interferers. We can therefore quantify the relative gain estimation bias introduced by the presence of interferers by

$$\begin{aligned} \frac{\Delta\mathbf{g}}{\mathbf{g}} &= \\ &= \frac{\mathbf{C}\left(\widetilde{\mathbf{G}}\Sigma_{\text{int}}\widetilde{\mathbf{G}}^H\mathbf{w}_{\text{ref}} - \text{diag}\left(\mathbf{w}_{\text{ref}}\right)\text{vecdiag}\left(\widetilde{\mathbf{G}}\Sigma_{\text{int}}\widetilde{\mathbf{G}}^H\right)\right)}{\mathbf{C}\left(\widetilde{\mathbf{G}}\Sigma_{\text{c}}\widetilde{\mathbf{G}}^H\mathbf{w}_{\text{ref}} - \text{diag}\left(\mathbf{w}_{\text{ref}}\right)\text{vecdiag}\left(\widetilde{\mathbf{G}}\Sigma_{\text{c}}\widetilde{\mathbf{G}}^H\right)\right)}, \end{aligned}$$

where $\mathbf{C} = \mathbf{S}^{-1}\mathbf{W}^H$ and the divisions should be read as element-wise divisions. This ratio represents the inverse of

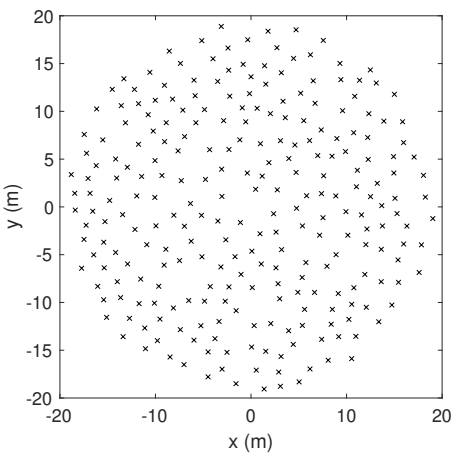

Figure 1. Station layout assumed in the simulations.

	beamformer setting	K	$\kappa(\mathbf{M})$
I	$l,m \in [-1,1], \Delta = 0.1$	441	$8.65 \cdot 10^3$
II	$l,m \in [-0.75,0.75], \Delta = 0.1$	256	$1.83 \cdot 10^4$
III	$l,m \in [-0.75,0.75], \Delta = 0.05$	961	$1.07 \cdot 10^4$
IV	$l,m \in [-0.5,0.5], \Delta = 0.05$	441	$2.99 \cdot 10^4$
V	$\mathbf{W} = \mathbf{I}$	256	257

Table 1. Beamforming scenarios used in the simulations.

the SIR in the context of a self-holography measurement. To get a useful expression for the SIR that can be used to assess the expected accuracy of self-holography calibration in a given context, it is convenient to make two simplifying assumptions. The first assumption is that the source is located at boresight, so that $\mathbf{w}_{\text{ref}} = \mathbf{1}$, i.e., a vector containing only ones. The second assumption is that the calibration converges reasonably well, so that $\mathbf{g}$ can be compensated with increasing accuracy over the iterations, so that we can assume $\mathbf{G} = \mathbf{I}$. Also note that, for a properly conditioned problem, $\mathbf{C}$ is invertible so that we can pre-multiply (regularise) both the numerator and denominator by $\mathbf{C}^{-1}$. Combined, this gives

$$\frac{\Delta\mathbf{g}}{\mathbf{g}} = \frac{\Sigma_{\text{int}}\mathbf{1} - \text{vecdiag}\,(\Sigma_{\text{int}})}{\Sigma_{\text{c}}\mathbf{1} - \text{vecdiag}\,(\Sigma_{\text{c}})} = \frac{1}{\text{SIR}}, \qquad (10)$$

where, as before, the divisions need to be interpreted as element-wise divisions.

4 Simulations

The inverse relationship between the relative gain estimation bias and the SIR was tested in simulations of a 38-m low-frequency aperture array station of the SKA operating at 100 MHz. The station layout is shown in Fig. 1. In these simulations, a calibration source with unit power was located at boresight in the presence of 1 to 5 interfering sources. These interfering sources were randomly placed with a radial position uniformly distributed between a direction cosine of 0.1 (to avoid confusion with the calibration source) and 1 and an azimuthal position uniformly

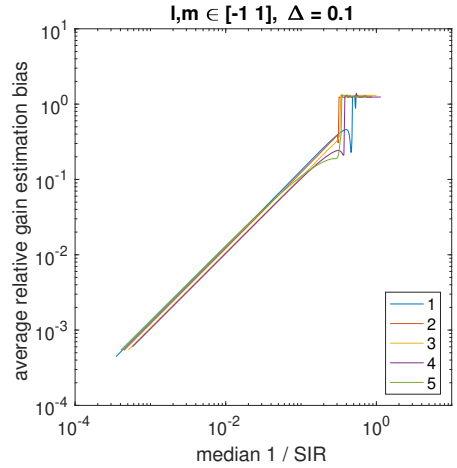

Figure 2. Average relative gain estimation bias versus the inverse of the median SIR for each of the 5 source models for beamforming scenario I.

distributed between 0 and 2π sr. The interfering sources had powers uniformly distributed between 0 and 1. The source covariance matrix of the interferers was scaled by a factor 0.01 to 19.81 in steps of 0.2 to test different SIRs for each source model. This whole exercise was repeated for five beamforming scenarios as listed in Table 1. The second column defines the grid of beams forms by specifying the interval and stepsize for the direction cosines l and m, except for the last scenario where $\mathbf{W} = \mathbf{I}$, i.e., the scenario in which the signal from the reference beam is correlated with the signal from the individual antennas. The third column shows the number of beams formed (K) and the last column gives the condition number of the measurement matrix, $\kappa(\mathbf{M})$.

Equation (10) presents the general case in which the SIR and, hence, relative gain estimation bias, may differ for different elements in the array. Although the averaging over each row of Σ_{int} described by $\Sigma_{\text{int}}\mathbf{1}$ signifies that not all elements may be equally affected by the interfering sources, depending on array and source geometry, for the random array and source geometry used in these simulations, it is usually reasonable to consider only the average relative gain estimation bias and average SIR. In these simulations, I encountered a few cases in which the specific source and array geometry produced an outlier in the SIR for some elements. For robustness to these outliers, I have therefore used the median SIR instead of the mean SIR. Figure 2 shows the results for all five source models for the first beamforming scenario. These results clearly show the inverse relationship between the relative gain estimation bias and the SIR.

Figure 3 shows the results for all five beamforming scenarios with three interfering sources present. It should be noted that a new set of three interfering sources was generated for each scenario, i.e., the interfering source model is not the same for the five scenarios. Despite this difference, the average relative gain estimation bias is predicted very well by

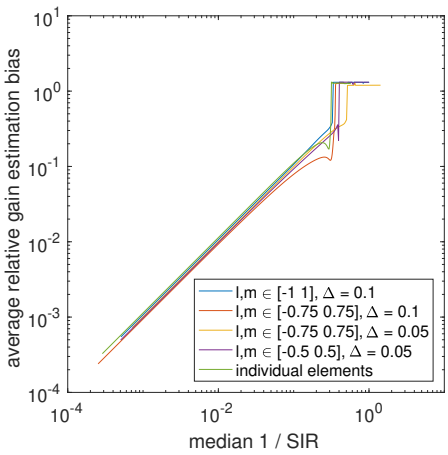

Figure 3. Average relative gain estimation bias versus the inverse of the median SIR for all beamforming scenarios listed in Table 1 with 3 interfering sources present.

the inverse relationship with the median SIR as calculated based on Eq. (10). This corroborates the generality of this expression and the intuition that $K = P$ is sufficient to make self-holography work.

Generalised self-holography provides a lot of freedom to set up the experiment by choosing various beamforming schemes. This begs the question how this may help. In general, a larger number of statistically independent measurements, for example multiple batches of beam measurements observed consecutively, will improve the precision of the gain estimates. If $K > P$, one can also ignore beams that are directly pointed at an interfering source in an attempt to improve robustness to this interfering source. On the other hand, a different choice for the grid of beams also has a significant effect on the condition number of the measurement matrix as indicated by the fourth column of Table 1. A higher condition number increases the susceptibility of the solution to noisy measurements. In that sense, self-holography based on correlation between the signal from the reference beam and the signals from the individual elements as considered in [2] is the best option among the beamforming scenarios considered here. It owes this low condition number to the orthogonality of the columns of the beamforming matrix $\mathbf{W}$. Several other matrices, including the matrix describing the discrete Fourier transform (DFT matrix), have the same attractive property. Although these matrices may not produce physically meaningful beams for a given array layout, they can be used to make superpositions of receiving element signals that may be highly suitable for self-holography.

5 Conclusions

In this paper, I presented a general formulation of the self-holography calibration method to capture variations of this method exploiting different beamforming schemes. Based on this formulation of the self-holography problem, an expression for the relative gain estimation bias due to the presence of interfering sources was derived. This expression indicates that this bias is inversely proportional to the signal-to-interference ratio (SIR) as defined in Eq. (10). This result was confirmed by simulations for various levels of interference, various randomly generated interfering source configurations and five different beamforming schemes. The generality of the derived expression implies that various beamforming options provide similar robustness to interfering sources. However, the chosen beamforming scheme has a significant impact on the condition number of the measurement matrix and therefore on the susceptibility to measurement noise. It is therefore recommended to choose a beamformer matrix consisting of (close to) orthogonal beamforming weight vectors, even if those do not provide phyiscally meaningful beams. Examples of such beamformer matrices are the identity matrix, in which each bemformer vector selects the signal from a single element, and the matrix describing the discrete Fourier transform (DFT matrix).

6 Acknowledgements

The author would like to thank Nelis Wilke and Jacki Gilmore for the fruitful discussions on the self-holography method. This work is supported by the Netherlands Organisation for Scientific Research.

References

[1] S. J. Wijnholds, “Calibration of Mid-Frequency Aperture Array Stations Using Self-holography,” in *2017 International Conference on Electromagnetics in Advanced Applications (ICEAA)*, Sep. 2017, pp. 967–970.

[2] C. R. Wilke, S. J. Wijnholds, and J. Gilmore, “Calibratability of Aperture Arrays Using Self-Holography,” *IEEE Transactions on Antennas and Propagation*, 2021, accepted for publication.

[3] M. P. van Haarlem *et al.*, “LOFAR: The Low Frequency Array,” *Astronomy & Astrophysics*, vol. 556, no. A2, pp. 1–53, Aug. 2013.

[4] P. E. Dewdney, P. J. Hall, R. T. Schilizzi, and T. J. L. W. Lazio, “The Square Kilometre Array,” *Proceedings of the IEEE*, vol. 97, no. 8, pp. 1482–1496, Aug. 2009.

[5] U. Kiefner, R. B. Wayth, D. B. Davidson, and M. Sokolowski, “Holographic Calibration of Phased Array Telescopes,” *Radio Science*, 2021, in preparation.